

## Oncologic angiogenesis imaging in the clinic: how and why?

The ability to control the growth of new blood vessels would be an extraordinary therapeutic tool for many disease processes. Too often, the promises of discoveries in the basic science arena fail to translate to clinical success. While several anti-angiogenic therapeutics are now US FDA approved, the envisioned clinical benefits have yet to be seen. The ability to clinically noninvasively image angiogenesis would potentially be used to identify patients who may benefit from anti-angiogenic treatments, prognostication/risk stratification and therapy monitoring. This article reviews the current and future prospects of implementing angiogenesis imaging in the clinic.

**KEYWORDS:** [<sup>18</sup>F]AH111585 • [<sup>18</sup>F]fluciclitide • [<sup>18</sup>F]galacto-RGD • angiogenesis • bevacizumab • cardiac disease • dynamic contrast-enhanced magnetic resonance • integrins • magnetic resonance • microbubbles • molecular imaging • nuclear medicine • oncology • targeted imaging • VEGF

Karen A Kurdziel<sup>†1</sup>,  
Liza Lindenberg<sup>1</sup>  
& Peter L Choyke<sup>1</sup>

<sup>1</sup>Molecular Imaging Program/Center for Cancer research, National Cancer Institute/National Institutes of Health, Bethesda, MD, USA

<sup>†</sup>Author for correspondence:  
Tel.: +1 301 443 0622  
Fax: +1 301 480 1434  
karen.kurdziel@nih.gov

### Angiogenic switch

The hypothesis that tumor growth is dependent on the development of new blood vessels and that the tumor cells themselves direct this process was proposed by Folkman in 1971 [1]. As tumors increase in size, they begin to exceed the approximate 1 mm oxygen diffusion limit, whereupon they must increase their blood supply in order to continue growing. Mechanisms by which they accomplish this includes angiogenesis, the process of developing new blood vessels from existing blood vessels. Tumors unable to undergo angiogenesis either die or arrest growth and remain in a dormant state that is typically less than 2 mm in diameter, resulting in large reservoirs of occult disease that potentially can activate under certain conditions, such as inhibition of the immune system or provocation by excess growth factors [1,2]. Angiogenesis plays a critical role in a tumor's continued growth. The proliferative rate of many dormant tumors is equal to that of angiogenic tumors; however, the apoptosis rate is significantly decreased in the latter. Thus, dormant tumors are poised for progression. While increased cellular proliferation and decreased apoptosis are necessary for tumor growth, they are not sufficient for sustained tumor growth. The evolution of an avascular 'dormant' tumor to an aggressive metastatic cancer is believed to occur after an 'angiogenic switch' has been thrown, giving the tumor the resources to obtain oxygen and nutrients through increased blood supply [3]. It

is projected that only approximately 1 in 600 'dormant' tumors switch to an angiogenic phenotype [4]. While the underlying trigger for the switch is not yet known and may differ according to tumor type, the process is directly regulated by oncogenes, tumor suppressor genes and indirectly controlled by the microenvironment (i.e., hypoxia, glucose concentration and pH). Udagawa *et al.* demonstrated that after transducing non-angiogenic osteogenic sarcoma cells with the *Ras* oncogene, the expression of the pro-angiogenic mediator, VEGF, increased by 38% and that of the anti-angiogenic factor thrombospondin-1 decreased by 50% [5]. In a mouse model, animals with *Ras* transduction lived only a few weeks, while those without the *Ras* oncogene lived for approximately 1 year. In general, activation of oncogenes often results in increased endothelial cell (EC) proliferation, migration and rate of tumor cell apoptosis.

Indirect control of angiogenesis by the microenvironment is illustrated by the the ability of a low oxygen environment to activate hypoxia-inducible factor (HIF)-1 $\alpha$ , which, in turn, activates pathways that among other things, control angiogenesis. HIF-1 $\alpha$  is a transcription factor that upregulates VEGF and other pro-angiogenic genes. HIF-1 $\alpha$  is degraded in the presence of oxygen, thus regulating angiogenesis under normal circumstances. If HIF-1 $\alpha$  is allowed to accumulate in the cell (either by increased production or decreased degradation), the cell will transcribe pro-angiogenic genes, resulting in angiogenesis.

future  
medicine part of fsg

### The players

Often lost in the discussion of angiogenesis is that it is a normal physiologic process and becomes pathologic only when it is no longer regulated. The biological process of angiogenesis is complex and involves activation of inflammatory cells (macrophages, monocytes and lymphocytes), the migration of endothelial or progenitor cells and the proliferation of existing ECs [6]. Angiogenesis plays a role in wound healing, the menstrual cycle and pregnancy. There are a multitude of regulatory molecules and pathways involved in angiogenesis, making therapeutic manipulation of the process challenging. These regulatory molecules may arise from within the extracellular matrix (ECM) or be produced by tumor, stromal or immune cells. For the most part, normal mature tissue is at a steady state: pro-angiogenic effectors balance anti-angiogenic effectors, resulting in no net increase in vascularity. Physiologically, under appropriate circumstances (tissue growth damage or repair), the balance is tipped resulting in angiogenesis.

While a complete description of the molecular pathways that play a role in angiogenesis is beyond the scope of this article (interested readers are referred to an excellent text on angiogenesis edited by Marmé and Fusenig [7]), selected well studied endogenous pro-angiogenic molecules are discussed briefly here and include: VEGF, FGF and  $\alpha_v\beta_3$  integrin.

#### ■ VEGF

VEGF is a 45-kD homodimeric glycoprotein that is secreted by tumor cells, and released and activated by heparinase, plasmin, urokinase and plasminogen. Its interaction with VEGF receptor-A on ECs results in the mobilization of circulating endothelial precursors, decreased apoptosis, increased vascular permeability and actin reorganization. Upregulated by the oncogene Ras, VEGF is secreted from tumors, and binds to VEGF receptor-1 (VEGFR-1) and -2 on ECs and bone marrow-derived cells. Therapeutic modulation of the VEGF system has been shown to potentiate chemotherapy and radiation effects.

#### ■ FGF

FGF is released by heparinase, associated with the ECM, and protected from degradation by binding to heparin sulfate proteoglycans. FGF induces cell proliferation, migration and production of proteases in ECs. Interactions with FGF receptors and heparin-like glycosaminoglycans result in FGF receptor dimerization or

oligomerization and activation of the receptor tyrosine kinase. This activates multiple transduction pathways including sustained activation of Ras [8]. One of the first angiogenesis inhibitors used in humans was low-dose IFN- $\alpha$ . A patient with progressive hemangiomas of both lungs leading to intractable hemoptysis was successfully treated with very-low-dose IFN- $\alpha$  [9]. At these low doses (below that needed for a cytotoxic or immunosuppressive effect), angiogenesis was inhibited by suppression of FGF [10].

#### ■ $\alpha_v\beta_3$ integrins

Integrins are a family of receptors within the ECM that span the cellular membrane, passing signals from the ECM to the cytoplasm and *vice versa*, essentially 'integrating' the intracellular cytoskeleton with the ECM. These adhesion molecules activate signaling pathways, which organize the cytoskeleton and increase cell proliferation.  $\alpha_v\beta_3$  integrins can be associated with proliferating ECs and malignant cells, but are not found in mature blood vessels.  $\alpha_v\beta_3$  integrin receptors contain a peptide binding pocket specific for the RGD (Arg-Gly-Asp) peptide sequence. RGD peptide binding can initiate a multitude of signaling pathways including those controlling gene expression, tissue development, inflammation, angiogenesis, tumor cell growth and metastasis.

High  $\alpha_v\beta_3$  expression has been demonstrated in melanomas, glioblastomas and certain sarcomas, with lower expression levels in breast cancers and renal cell carcinomas [11].  $\alpha_v\beta_3$  integrin levels have been correlated with disease progression in several malignancies including: melanoma, glioblastoma, ovarian cancer and breast cancer [12,13]. It has also been shown to mediate adhesive reactions of platelets and acts as a receptor for fibrinogen, von Willebrand factor and fibronectin [14].

### Why image?

As the treatment of cancer moves towards the molecular control of cancer using targeted therapies, conventional anatomic imaging may prove insufficient. The current reliance on size criteria alone in determining whether a drug is effective can take many months. Moreover, determining activity within a tumor that is stable in size is impossible when using size criteria alone. Anti-angiogenic therapeutics targeting various steps in the angiogenesis pathway have entered the clinic [15] (i.e., bevacizumab, an antibody which neutralizes VEGF [16], sunitinib, which blocks VEGF receptors on vessels [17], and cilengitide,

which blocks binding to integrins [18]). As the molecular changes occurring with anti-angiogenic treatment are not expected to result in rapid tumor volume loss, an imaging biomarker of therapeutic response could be of great value. Angiogenic inhibitors appear to have a biphasic (U-shaped) dose–response curve: while their effect initially increases with dose, administration of higher doses actually results in a decreased response [19]. Optimal dose and dosing schedules could be defined if one had an accurate marker for therapeutic response. Additionally, many angiogenic inhibitors appear to negatively regulate angiogenesis for a while before alternate molecular pathways develop to promote angiogenesis [20]. The point at which tumors begin to become resistant to angiogenic inhibition would be a useful marker for understanding the degree and duration of angiogenic suppression.

Angiogenesis is the key to a tumor's independence. While it entails a complicated interaction of numerous effectors and pathways, control of this process may enable us to establish 'permanent' tumor dormancy. *A priori* identification of the predominant signaling pathways could have prognostic value and may guide therapeutic selection. The ability to monitor the process *in vivo* can help direct such interventions.

### How to image

There are several clinical imaging tools available, which can indirectly image angiogenesis by evaluating blood flow and perfusion. A growing number of imaging agents are being used to directly image angiogenesis by aiming at specific targets.

#### ■ Indirect imaging of angiogenesis

There are several methods of indirectly monitoring angiogenesis using conventional imaging, notably, contrast-enhanced ultrasound (US), CT and MRI.

Routinely performed contrast-enhanced MRI and CT allow for the subjective differentiation between areas that are 'well perfused' and those with 'low or no' perfusion. The contrast agents used in both modalities highlight arterial blood flow initially, rapidly followed by venous and blood pool and extravascular diffusion. Since these agents are low in molecular weight, they readily leak from angiogenic vessels making it difficult to distinguish between intravascular containment and extravascular leakage. For typical clinical applications, 'snapshot' images from arterial and venous phases are sufficient for diagnostic purposes, however, to attempt

to quantify perfusion and vessel permeability, dynamic contrast-enhanced (DCE) methods are used. Dynamic contrast imaging collects sequential images over a period of time and can be used to monitor perfusion and permeability in select clinical trials.

#### ■ Dynamic contrast-enhanced MR

With the evolution of faster MRI sequences, rapid sequential imaging following a controlled intravenous bolus injection of a low-molecular-weight gadolinium diethyltriamine pentaacetic acid (Gd-DTPA) based contrast agent is now feasible and widely available [21]. This dynamic imaging captures the entire time course of contrast enhancement in an area of interest. By drawing a focal region of interest (ROI) and applying it to each image in the time series, a time activity curve (TAC), from which parameters representing the kinetics of the blood flow and permeability, can be extracted. As Gd-DTPA-based contrast agents do not enter the intracellular space to a significant extent, the resultant TAC can be fit to a two compartment kinetic model, representing transit to and from the vasculature and extravascular extracellular spaces. For DCE MRI, the rate constant describing the transit of contrast agent from the blood into the extravascular extracellular space is often referred to as  $K^{\text{trans}}$  and the rate constant describing the return of tracer (from the extracellular extravascular space) to vasculature is termed  $k_{\text{ep}}$ . Parametric maps can be created resulting in images where the image intensities can be colorized and made proportional to the magnitude of the rate constants,  $K^{\text{trans}}$  or  $k_{\text{ep}}$  [22]. It can be seen from FIGURE 1 that high  $K^{\text{trans}}$  (rapid influx into extravascular tumor space) and  $k_{\text{ep}}$  (the rate of tumor efflux) is associated with tumor phenotype. While modeling can be performed assuming the contrast entrance into the blood is instantaneous, a more realistic model incorporates the rate at which blood initially enters the system, using the vascular input function (estimated from an ROI within a homogenous portion of a vessel in the field of view). In theory, the use of an arterial input function results in more accurate parameter estimates [23]; however inclusion of an arterial input function also risks the introduction of new errors from flow-based artifacts in the targeted vessel [24]. Initial single center clinical trials using DCE MRI are promising, with visible changes in parameters between baseline and early post-therapy scans (FIGURE 2) [25]. The clinical relevance of these findings has yet to be validated particularly in light of a recent study

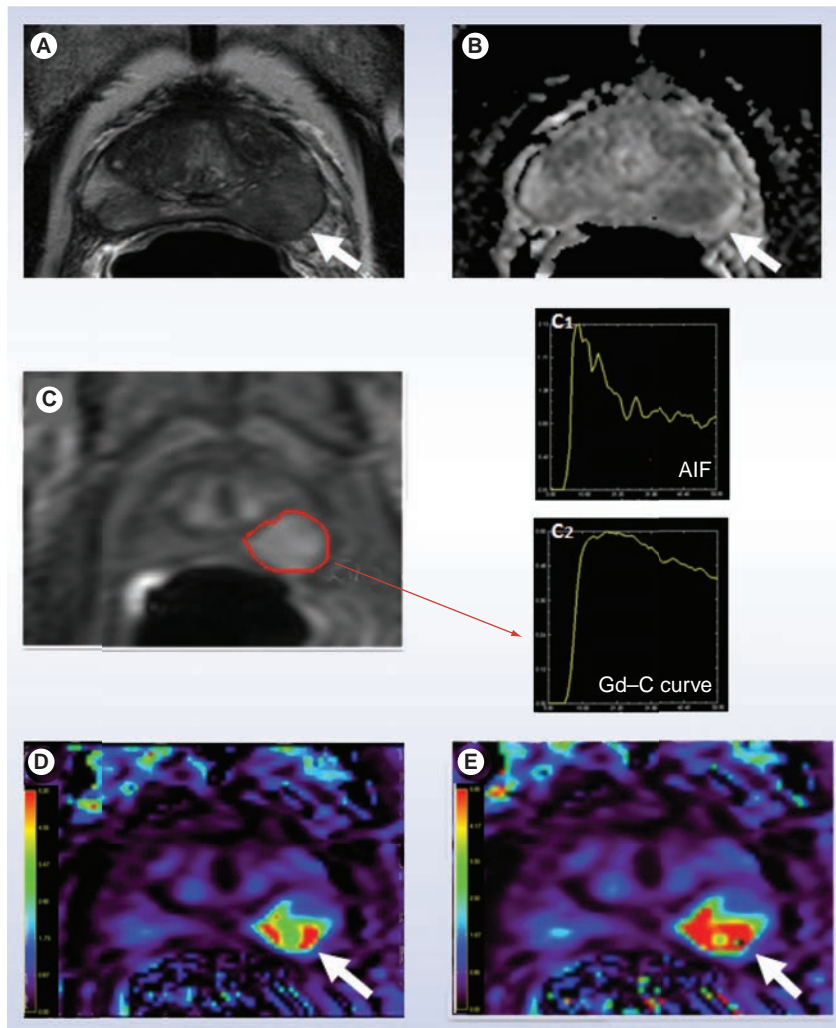


**Figure 1.** Axial  $T_2$ -weighted MRI of a 65-year-old man with serum prostate-specific antigen of 9.2 ng/dl shows a vague low signal intensity lesion in the left mid-base peripheral zone (arrow). (A) Apparent diffusion coefficient map derived from diffusion-weighted MRI shows restricted diffusion within the left peripheral zone lesion (arrow). (B) Raw dynamic contrast-enhanced MRI demonstrates fast and early enhancement within the left peripheral zone lesion (marked in red). (C)  $C_1$ : Arterial input function curve;  $C_2$ : Gd C curve of the left peripheral zone lesion;  $K^{trans}$  (D) and  $k_{sp}$  (E) maps derived from dynamic contrast-enhanced MRI also localizes the left peripheral zone lesion (arrow). AIF: Aortic input function; C: Concentration; Gd: Gadolinium. Image and legend courtesy of Baris Turkey, MD, Molecular Imaging Program, NCI, USA.

showing higher morbidity in patients receiving anti-angiogenic therapy (compared with chemotherapy alone) [26,27].

Dynamic contrast-enhanced MRI provides the potential for semiquantitative assessment; however, the methodology first needs to be standardized if it is to be widely used and results are to be compared across centers [28,29]. Given the multiple vendors of MRI imaging equipment, the vast range of available scanning sequences and coils, and wide variability in compliance, standardization is not a simple process. One simplified method, which avoids the pitfalls of two

compartment modeling, involves normalizing the magnetic resonance signal intensity of the postcontrast images to baseline, thus establishing a relationship between signal intensity and contrast agent concentration (i.e., each study serves as its own control); however, the results are still semiquantitative and the changes in signal intensity are not linear over the range of concentrations of gadolinium or background  $T_1$  values, and therefore require further calibration.

There is significant ongoing effort to validate and standardize DCE MRI. This work requires meticulous quality control and assurance, determination of parameter reproducibility, standardized imaging procedures and image analysis, and, most importantly, correlation with an existing biomarker (i.e., proof that the process being measured actually represents the process of interest). Such requirements have made accrual to trials with DCE MRI difficult and cast doubt on the ability to actually recruit patients and conduct multi-institutional trials with rigid quality control, which hitherto has been lacking in radiology departments.

Routinely used low-molecular-weight Gd-DTPA-based imaging agents cannot be used to measure vascular volume since they easily leave the vasculature, diffusing into extravascular spaces. Complexing gadolinium with albumin, dextran, liposomes and dendrimers, for example, results in macromolecular contrast agents that remain confined to the vasculature at least for the period of the scanning, or enter the extravascular space only when the vessels are highly permeable; such agents may provide a method for measuring vascular volume in the future.

### ■ Ultrasound

Ultrasound relies on acoustic reflections in soft tissue to construct an anatomic image. Contrast-enhanced US is an appealing imaging modality for several reasons. US scanning equipment offers portability and low cost and data acquisition is rapid and in real time. Additionally, sound waves lack ionizing radiation, which is advantageous for patient safety over repeated examinations.

Doppler US can measure the velocity of blood, indicate flow direction and estimate blood flow [30]. Color Doppler can delineate tortuous vascular anatomy and malformations, and help assess anti-angiogenic effects of therapy on tumors. Unfortunately, this technique is limited by variations in flow velocity from the cardiac cycle and slow capillary flow, which if less than 1 mm/s cannot be detected. Power Doppler is

an improved feature that increases sensitivity at low flow rates and is not angle dependent. Blood volume flow can be calculated by this method, but there is no standardization [31]. Key features of power Doppler include better edge definition and depiction of flow continuity [32]. The vascularity index is a quantitative parameter developed to assess *in vivo* tumor angiogenesis and is the ratio of the number of coloured pixels in the ROI divided by the total number of pixels in that ROI. Chen *et al.* demonstrated that the vascularity index was associated with tumor differentiation, lymph node metastasis and patient survival in colon cancer in one study and with lymph node metastasis, combined VEGF and PIGF expression status and patient survival in another study of gastric cancer [33,34]. Resistance to blood flow in the microcirculation can be determined with Doppler in tumors, but mixed high and low flow rates are often found secondary to characteristics of the tumor and compensatory response of surrounding tissue. Certain tumors, such as choriocarcinoma, demonstrate a consistent low resistance index that can be used to monitor effects of chemotherapy [35]. Power Doppler still has significant limitations. The resolution obtained with high frequencies restricts evaluation to only superficial tissue. Convoluted small vessel distribution is also difficult to distinguish. Vessels less than 100  $\mu\text{m}$  in diameter and blood flow rates less than 1 mm/s (e.g., in the capillaries) are still challenging to evaluate and can be complicated by respiratory or cardiac motion artifact [36]. The combination of contrast-enhanced US and power Doppler methods has been used to increase microvessel detection. In a preclinical mouse study with human breast cancer xenografts, contrast-enhanced Doppler US correlated with angiogenic activity evaluated by immunohistochemistry in vessels measuring approximately 40  $\mu\text{m}$  in diameter [37]. Advanced Doppler systems, including contrast-enhanced harmonic and pulse inversion imaging, may enhance small vessel flow imaging.

Contrast agents refine these signals through backscatter or reflection of sound characterized by their chemical shape and size. Microscopic liposomes, nanoparticle emulsions and microbubbles are examples of the contrast agents that have been used [38]. When gas-containing microbubbles are injected, they are confined to the vascular space owing to their size. The insonating pressure wave creates reverberations on the microbubble that are transmitted back to the receiver at harmonic frequencies that uniquely identify the microbubble as the source of the

returning sound waves. This results in a very high target:background ratio. Microbubble sizes range from 1 to 4  $\mu\text{m}$  (the largest imaging agent in use in humans) and the basic design is an inert gas-filled core, typically perfluorocarbon, and an outer shell of albumin, lipid or biopolymers. With low US transmission frequencies, the nonlinear oscillation of microbubbles produces an acoustic signal that separates it from the background tissue. A high contrast:tissue background

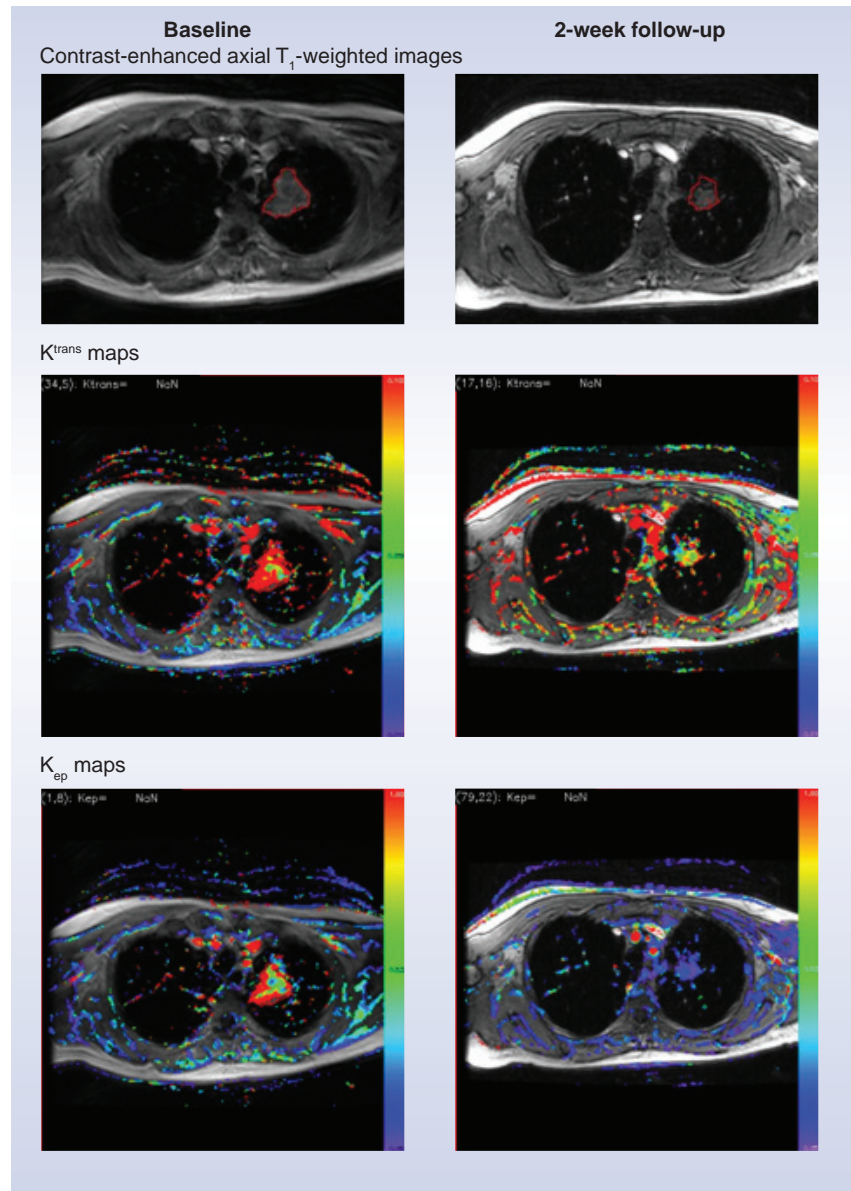


**Figure 2. A 57-year-old male with nonsquamous cell lung cancer lesion in the upper lobe of the left lung (region of interest shown by red coloring).** Initially high  $K^{\text{trans}}$  and  $k_{\text{ep}}$  are seen in the baseline parametric maps, with the red coloring representing high flow (right column, second and third rows). Following sorafenib treatment, the lesion size decreased and the  $K^{\text{trans}}$  and  $k_{\text{ep}}$  values are reduced. Image and legend courtesy of Baris Turkey, MD, Molecular Imaging Program, NCI, USA.

ratio results in highly sensitive detection (even one microbubble can be identified) and quantification of these signals is becoming possible. Microbubbles are administered intravenously and, once degraded, the encapsulated gas is exchanged through the lungs. They can be purposely destroyed by high-power US to facilitate repeated measurements in a single field of view. To improve their stability and residence times in circulation, polymers such as polyethylene glycol (PEG) can be attached to the microbubble surface. Microbubbles are similar in size to red blood cells and are confined intravascularly making them uniquely suited to assess blood flow and also target ECs.

Published literature is scarce on indirect angiogenesis imaging in human studies assessing anti-angiogenic therapy with US. Lassau *et al.* showed that microbubble activity corresponds to response in metastatic renal cell carcinoma patients treated with an anti-angiogenic medication [39]. Larger studies are necessary for further validation.

Microbubbles can also be labeled with molecular ligands such as antibodies or peptide binding ligands. Because the microbubble is already so large, the addition of antibodies or peptides to the surface of the microbubble does not change the pharmacokinetics, as it might with smaller carrier molecules. Molecular-targeted microbubbles for angiogenesis have focused on targeting integrins and growth factor receptors with promising applications in detection and monitoring therapy response.

#### ■ Nuclear medicine/PET

The main advantage of radionuclide imaging is its potential for high specificity. Limitations of nuclear imaging include long acquisition times, the increased potential for motion artifacts and low spatial resolution. Future improvements in camera technology may decrease these limitations. The radiation doses are similar and generally less than that of diagnostic CT.

Another imaging method that could be applied to angiogenesis is quantitative blood flow imaging using  $^{15}\text{O}$ -water PET [40]. The major limitation of its use is the availability of the imaging agent ( $t_{1/2}$  = approximately 2 min, requiring an onsite cyclotron) and subsequent complicated imaging procedure. Since  $^{15}\text{O}$  water is completely diffusible (i.e., freely transfers between the extra- and intracellular spaces), the TACs derived from the dynamic images (analogous to DCE MRI) can be fit to a two compartmental model. For brain imaging, the

initial uptake of  $^{15}\text{O}$ -water ( $k_1$ , analogous to  $K^{\text{trans}}$  in DCE MRI) is used to measure flow, while for tumor and cardiac imaging, blood flow is modeled using the efflux ( $k_2$ , analogous to  $k_{\text{ep}}$  in DCE MRI) portion of the curve and parametric images of  $k_1$  and  $k_2$ , can be made. Since the activity measured in tissues directly corresponds to the injected activity, quantitative blood flow measurements can be readily made. Like all PET imaging studies, the resolution of such studies is inferior to CT and MRI and that, combined with its limited availability and complexity, has led to limited usage.

Blood volume can be measured with  $^{11}\text{C}$ -CO- or  $^{15}\text{O}$ -PET. CO binds tightly to red blood cells, which, in turn, are distributed uniformly throughout the vasculature. The volume fraction of blood in tissue can be determined by dividing the concentration within the ROI by the concentration in the blood. The measurement of CO uptake on the PET images, combined with the hematocrit ratio (estimated to be 0.85 by Grubb *et al.* [41] permits quantitative calculation of the blood volume. Again, limited by the short half-life of the  $^{11}\text{C}$  positron emitter ( $^{11}\text{C}$  ~20 min) these studies need to be performed near a cyclotron. An additional procedural hurdle is that the tracer is administered as a gas (CO), requiring special room ventilation owing to the potential toxicities of CO.

Myocardial perfusion imaging has been extensively developed to study coronary artery disease in the heart. In theory, such methods can be applied to angiogenesis imaging. Routinely used cardiac perfusion agents include  $^{201}\text{Tl}$  chloride,  $^{99\text{m}}\text{Tc}$ -tetrofosmin, sestamibi (SPECT) or  $^{82}\text{Rb}$  (less commonly  $^{13}\text{N}$  ammonia) PET/CT. Each of these have been used in tumor imaging with limited success due to their extraction from the blood and subsequent specific and nonspecific cellular interactions, resulting in variations in background activity and distributions not distinctly representative of tumor perfusion. If an intravascular radiolabeled imaging agent that does not significantly accumulate in the lungs or reticuloendothelial system were available, nuclear tumor perfusion/blood volume imaging may be more widely used.

#### Direct imaging of angiogenesis

As indirect measures of blood flow and permeability are not specific markers for angiogenesis and may represent other processes (i.e., infection, inflammation or vascular dilatation), significant efforts are being put forth to create imaging agents that specifically image angiogenesis.

### ■ Targeted radionuclide imaging

As mentioned previously, the RGD binding pocket of integrin is important for downstream activation of angiogenesis. Angiogenic vessels are rich in integrins and, as a consequence, can be targets for molecular imaging. Multiple imaging agents based on the RGD amino acid sequence motif have been successfully developed and tested in animal models of angiogenesis [42–45] and several RGD-binding PET agents have entered human clinical trials.

One such promising RGD-binding PET agent is the glycosylated cyclic pentapeptide  $^{18}\text{F}$ -galacto-RGD, which was developed by conjugating the RGD containing cyclic pentapeptide cyclo(Arg-Gly-Asp-dPhe-Val) with galactose-based sugar amino acids. PET imaging allows specific imaging of  $\alpha_v\beta_3$  expression and the uptake of  $^{18}\text{F}$ -galacto-RGD correlates with  $\alpha_v\beta_3$  expression in tumor xenografts as well as in patients. Successful human  $\alpha_v\beta_3$  integrin imaging with  $^{18}\text{F}$ -galacto-RGD has been demonstrated in invasive ductal breast cancer and squamous cell head and neck cancer, sarcoma, melanoma and glioblastoma. The resultant standardized uptake value (SUV) and tumor:background ratios correlated with integrin immunohistochemistry and  $\alpha_v\beta_3$  expression, and was shown to be high and variable in primary tumors as well as in metastases [11,44,46–50].  $^{18}\text{F}$ -galacto-RGD has also been used to provide evidence of myocardial angiogenesis following a transmural infarction in humans [51]. While initial results are promising, its synthesis is long and complicated, potentially slowing its clinical translation.

$^{18}\text{F}$ -fluciclatide ( $^{18}\text{F}$  AH111585), a synthetic cyclic peptide containing the RGD tripeptide which preferentially binds with high affinity to  $\alpha_v\beta_3$  integrins is also under clinical investigation. Early studies have shown it to be safe and 'imageable' in patients with breast cancer, with favorable dosimetry [52].

An ongoing proof-of-concept study aimed at correlating  $^{18}\text{F}$ -fluciclatide uptake with  $\alpha_v\beta_3$  integrin levels in tumors is underway. Preliminary data show variable intratumoral distributions. FIGURE 3A shows a melanoma with diffuse uptake ( $\text{SUV}_{\text{max}}$  6.4), while FIGURE 3B shows a metastatic melanoma focus in a different patient in which only the rim of the tumor shows uptake ( $\text{SUV}_{\text{max}}$  of 3.0).

Several other integrin-targeted agents are under development with attempts to improve specificity and biodistribution to increase the tumor:background ratio. While still in the preclinical stages,  $^{64}\text{Cu}$ -1,4,7,10-tetra-

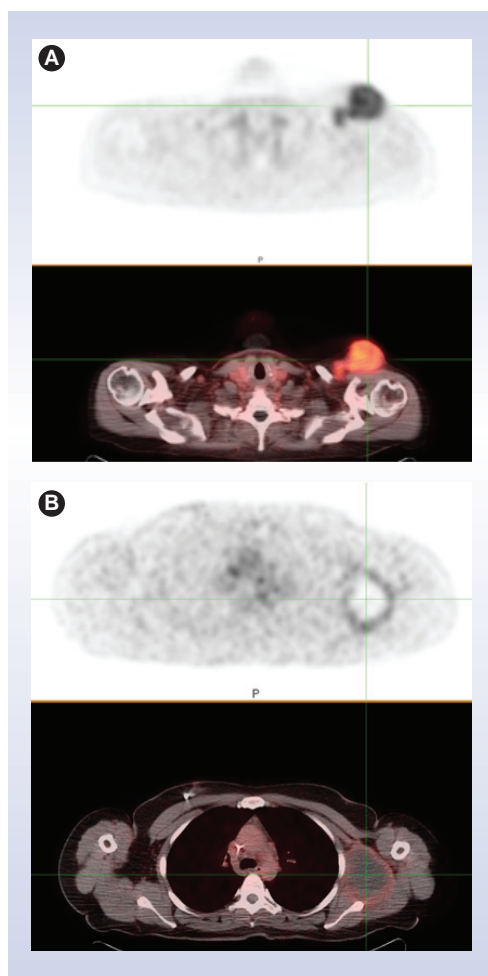


**Figure 3. Images of  $\alpha_v\beta_3$  integrin PET/CT imaging performed after injection of  $^{18}\text{F}$ -fluciclatide in two patients with melanoma. (A) Diffuse high uptake ( $\text{SUV}_{\text{max}}$  6.4) in the large soft tissue metastasis can be seen (cross hairs). (B) The metastatic melanoma focus shows a central photon deficit and mild ( $\text{SUV}_{\text{max}}$  of 3.0)  $^{18}\text{F}$ -fluciclatide uptake around the periphery.**

azacylododecane-N,N',N'',N'''-tetraacetic acid (DOTA)-knottin ( $^{64}\text{Cu}$ -DOTA-knottin 2.5F) is a peptide engineered for integrin binding. Binding the RGD receptor with high affinity (low nmol/l range), its low background activity may enable improved detection of lung tumors. Nielsen *et al.* showed intense uptake in lung metastases in a transgenic mouse model FIGURE 4, with tumor:background ratios ranging from 3.3 to 8.3, enabling the detection of metastatic lesions as small as 2.5 mm [53].

Extensive work on the development of radio-labeled imaging agents targeting VEGF is also underway. Nuclear imaging using antibodies to VEGF has been successfully employed in pre-clinical models using both PET and SPECT radionuclides, including  $^{99\text{m}}\text{Tc}$ ,  $^{111}\text{In}$ ,  $^{89}\text{Zr}$ ,  $^{64}\text{Cu}$

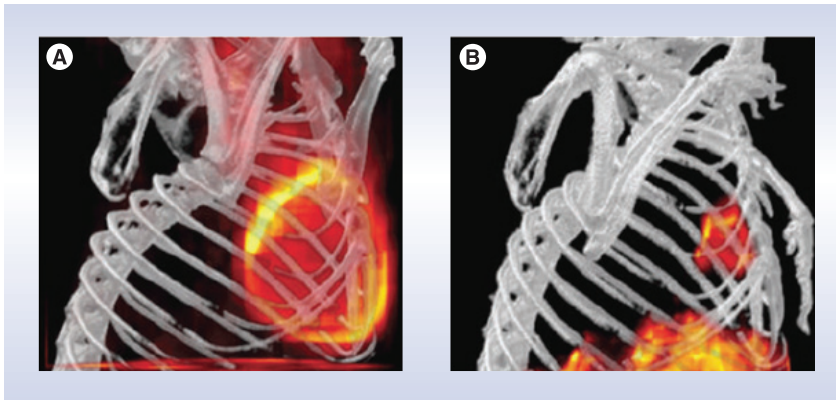


**Figure 4. A PET/CT volume rendering of a mouse thorax, imaging glucose metabolism (A) and  $\alpha_v\beta_3$  integrin expression (B).** A lung nodule obscured by physiologic cardiac uptake on the  $^{18}\text{F}$ FDG (B) image is clearly visualized in the  $^{64}\text{Cu}$  knottin 2.5F (A) image. Activity beneath the diaphragm represents physiology activity. Reproduced with permission from [53].

and  $^{86}\text{Y}/^{90}\text{Y}$ . Preclinical SPECT imaging with  $^{111}\text{In}$  VEGF<sub>121</sub> and VEGF<sub>165</sub> radiotracers was reported by Wagner *et al.* [54]. VEGF<sub>121</sub> has also been labeled with  $^{64}\text{Cu}$  ( $t_{1/2} = 12.7$  h), a positron emitter yielding increased sensitivity and potentially quantitative monitoring of angiogenesis and VEGFR expression. Micro-PET imaging with  $^{64}\text{Cu}$ -DOTA-VEGF<sub>121</sub> exhibited nanomolar receptor-binding affinity. In a small U87MG glioblastoma tumor with high VEGFR-2 expression, there was intense, rapid and specific uptake [55]. Willmann *et al.* monitored the biological response to hindlimb ischemia with  $^{64}\text{Cu}$ -DOTA-VEGF<sub>121</sub> in mice and showed the angiogenic response to be greater in exercised than nonexercised mice [56]. The kinetics of  $^{64}\text{Cu}$ -DOTA-VEGF<sub>121</sub> uptake in a rat model of myocardial infarction was imaged by Rodriguez *et al.* [57]. By radiolabeling the anti-angiogenic drug bevacizumab with  $^{89}\text{Zr}$  and  $^{111}\text{In}$ , Nagengast *et al.* imaged VEGF expression in mouse models [58]. More recently, the same group radiolabeled the anti-angiogenic drug ranibizumab with a monoclonal antibody fragment derived from the same parent murine anti-VEGF antibody and showed that sunitinib decreases  $^{89}\text{Zr}$ -ranibizumab tumor uptake, most notably in the tumor center, with a marked rebound after discontinuation of the anti-angiogenic therapeutic agent [59].

An exciting area of research involves the combination of an imaging agent with a therapeutic agent, creating a so-called 'theranostic agent'. This would allow visualization of the target, quantification of the drug delivered to the target and therapeutic monitoring using just a single agent. The potential for a combined imaging

and radiotherapy agent was reported by Nayak *et al.* [60] who developed the radioimmunoconjugate  $^{86}\text{Y}$ -CHX-A'-DTPA-bevacizumab, which could serve as a surrogate imaging marker for therapeutic  $^{90}\text{Y}$  CHX-A'-DTPA-bevacizumab. Biodegradable integrin-targeting dendritic PET nanoprobe have been developed for the non-invasive imaging of angiogenesis. Preliminary data showed them to have a 50-fold enhanced binding affinity when compared with monovalent RDG peptides. The biodegradable nature of these particles should reduce potential toxicities by promoting renal excretion, thereby reducing exposure time in the body. Its modular nature allows control of its blood circulation time and route of excretion (both highly dependent on molecule size) due to the ability to alter dendritic branching and polyethylene glycol length, and to "switch out" the targeting moieties (i.e., target VEGF or other entity instead of integrins). It also permits attachment of a variety of radiohalogens (e.g., iodine, bromine and astatine) used in both imaging and therapy. This nanoprobe could potentially have implications in both therapy and imaging (FIGURE 5) [61].

#### ■ Targeted US

Targeted microbubbles for US, based on monoclonal antibodies and ligands such as the snake venom disintegrin, echistatin, which contains the RDG sequence, have also been used to detect integrins. Murine studies targeting tumor angiogenesis with these contrast agents have yielded strong US signals specific to new vascular growth [62,63]. Knottin is a peptide that binds to  $\alpha_v\beta_3$  integrins and offers improved peptide and microbubble stability. Willmann *et al.* demonstrated increased US signals in mouse models of human ovarian adenocarcinoma with knottin microbubbles, which correlated strongly to tumor vasculature [64].

Dual or multitargeted microbubbles have two or more ligands specific for different angiogenic targets with the expectation that this will increase the probability for binding to new proliferative vessels. This was recently tested in human ovarian cancer xenografts in mice using microbubbles labeled with antibodies to VEGFR2 and integrin  $\alpha_v\beta_3$ . Increased tumor vessel attachment was noted in the dual-targeted microbubble compared with single-targeted microbubbles [65].

VEGF-specific targeting moieties can also be integrated into US contrast agents. Targeted US contrast agents can be prepared by attaching a molecular complex to a microbubble through

noncovalent bonds. These attachments can be on the PEG arm, which can also serve as a molecular spacer. Ligands can also be directly integrated into the microbubble shell. The biotin–streptavidin link (noncovalent) has been the most common route of attachment in animal studies, but its clinical usefulness is limited by its potential immunogenicity. Maleimide reactive groups can be added to the microbubble surface and conjugated to thiol ligands by thioether bonding, thus reducing the immunogenic response. Anderson *et al.* linked *scVEGF* to microbubbles through thioether covalent bonds. Targeting the VEGF receptor (VEGFR)-2, mouse models of colon adenocarcinoma demonstrated affinity for tumor vasculature on US [66]. Myrset *et al.* also utilized the thiol-maleimide couplings to attach peptides to microbubbles targeting the angiogenic marker, VEGFR2, and the inflammatory marker, E-selectin, with successful results [67]. Exploring other chemical couplings of ligands such as amine (NH<sub>2</sub>)/amide attachments are additional options in developing targeted microbubbles that minimize the risk of immunogenicity [68]. Such efforts will facilitate translation into the clinical setting.

Microbubble studies examining response to anti-angiogenic therapy have shown significant changes that precede visible anatomic changes

in the tumor. Kinase insert domain receptor is a binding lipopeptide analogous to VEGFR-2 that can be directly inserted into the microbubble shell. Pysz *et al.* used murine models of human colon cancer treated with anti-VEGF therapy and found decreases in US signal when compared with baseline exams using kinase insert domain receptor-targeted microbubbles. Findings were evident in mice treated with anti-angiogenic therapy as early as 24 h after the start of treatment and decreased by approximately 46% [65]. There are no reports, at the time of writing, of using molecular angiogenesis-targeted imaging agents for US in patients.

Research has also focused on US contrast agents as vehicles for drug delivery. Drugs can be complexed to the lipid shell and selectively released when the contrast agent is destroyed by US signals at specific sites. Drug-loaded contrast agents have been developed for a variety of applications but the majority has focused on chemotherapeutic delivery for treatment of tumor angiogenesis. Several animal and *in vitro* studies have shown decreased systemic toxicity and increased potency at targeted locations. Specific to angiogenesis treatment, animal models have shown marked attenuation of tumor growth after delivery of chemotherapy by US contrast agents [38].

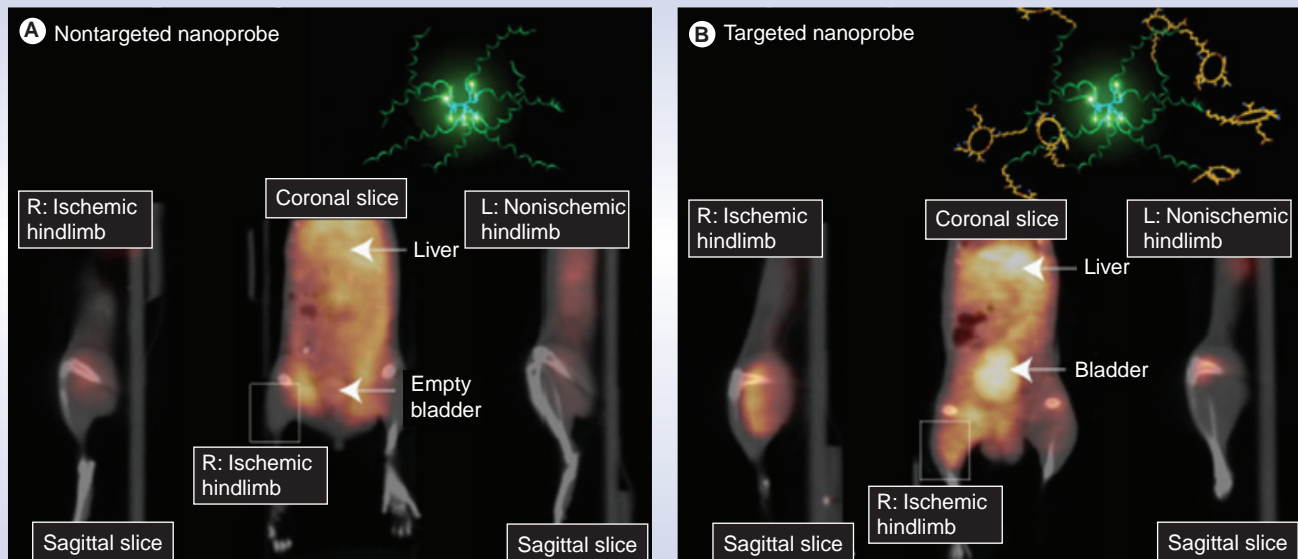


**Figure 5. Noninvasive PET/CT images of angiogenesis induced by hindlimb ischemia in a murine model. (A)** Nontargeted dendritic nanoprobe. **(B)** Uptake of  $\alpha_v\beta_3$  integrin-targeted dendritic nanoprobe. Note accumulation of  $\alpha_v\beta_3$  integrin-targeted dendritic nanoprobe in the right ischemic hindlimb (box in **[B]**), when compared with the lack of uptake of the nontargeted agent (box in **[A]**). The structure and biodegradable nature of this nanoprobe may make it useful in developing a nontoxic, targeted combined therapy/imaging agent.

L: Left; R: Right.

Modified with permission from [61].

### ■ Targeted MRI

Attempts to measure angiogenesis directly with MRI have been met with limited success. Several imaging agents have been evaluated in preclinical models only. An approach using liposomes (diameter of 300–350 nm) containing  $Gd^{3+}$  and targeted using the  $\alpha_v\beta_3$  specific antibody LM609 showed promise but has not been developed further [43].

A major drawback to using MRI in this setting is its limited sensitivity (detected at millimolar levels) and it is technically challenging to label nanoparticles with large amounts of Gadolinium. In the future, this limited sensitivity of MRI might be overcome by signal amplification strategies that generate higher target to background contrast [69]. Hyperpolarized  $^{13}C$  MRI also holds promise for much greater sensitivity, although the hyperpolarization process is difficult to generate and suffers from a short (2–3 min) half-life.

### Future perspective

Angiogenesis is an integral component of tumor development and tissue remodeling. The ability to noninvasively detect and monitor this process has numerous potential clinical applications. A successful targeted imaging agent could potentially be used to identify patients who may benefit from anti-angiogenic therapies, to monitor anti-angiogenic therapy, to identify sites of high angiogenesis for focal therapies or to provide prognostic information. There are numerous clinical options for indirect measurement of angiogenesis, by measuring blood flow and perfusion as surrogates, but these parameters can be affected by processes other than angiogenesis, notably inflammation. For this reason, a more targeted approach is preferable.

As the process of angiogenesis involves a complicated dynamic interplay among numerous modulators, information about the system determined at a single time point is not likely to be

#### Executive summary

- As tumors increase in size, they begin to exceed the approximate 1 mm oxygen diffusion limit; to continue growing they must increase their blood supply.
- They accomplish this by increasing or developing new blood vessels. This is called angiogenesis, a physiological process under tight control by numerous regulatory molecules and signaling pathways.
- In the absence of angiogenesis, small tumors either become necrotic or become dormant (proliferation continues; however, it is balanced by apoptosis, resulting in no net growth).
- Under the appropriate conditions, an 'angiogenic switch' may be thrown, resulting in increased pro-angiogenic factors and upregulation of angiogenesis. This appears to be the turning point in the tumor's ability to be self-sufficient and eventually to metastasize.
- Noninvasive identification of which tumor foci have this capability could help direct therapy, provide prognostic information and provide a therapeutic opportunity. This can be done indirectly by measuring perfusion/blood flow or directly using targets imaging agents.

#### The players

- Amongst the complicated interplay of angiogenic modulators, VEGF and integrins are the most studied as potential targeting platforms.
- High  $\alpha_v\beta_3$  integrin expression has been demonstrated in numerous cancer types and this expression has been correlated with disease progression in several malignancies.
- Activation of the VEGF receptor results in initiation of several pro-angiogenic signaling pathways and its modulation has been shown to potentiate chemotherapy and radiotherapy effects.

#### Why image?

- As the treatment of cancer moves towards the molecular control of cancer using targeted therapies, conventional anatomic imaging may prove insufficient.
- Anti-angiogenic therapeutics targeting various steps in the angiogenesis pathway are entering the clinic with mixed response.
- Angiogenic inhibitors appear to have a biphasic (U-shaped) dose–response curve: while their effect initially increases with dose, administration of higher doses actually results in a decreased response. Optimal dose and dosing schedules could be defined if one had an accurate marker for therapeutic response.

#### How to image

- Indirect imaging:
  - Clinically available methods to image blood flow and perfusion using radiolabeled drugs and contrast CT, MRI and ultrasound (microbubbles).
- Direct imaging:
  - Targeted imaging agents (predominantly integrins and VEGF) are being developed for MRI, ultrasound and nuclear/PET imaging. Most are in the preclinical phase.
  - Two promising radiotracers are in Phase I/II studies in humans and at least one will likely translate to the clinic in the next decade.

#### The next steps

- Angiogenesis plays a key role in the establishment of life-threatening tumors and noninvasive detection/monitoring of this process is essential.
- Once accurate and specific targeting is established the development of a combined therapy/diagnostic platform offers the potential to select, properly dose and monitor patients with therapies directed at angiogenesis.

representative of the entire state of the angiogenic pathway. Targeted molecular imaging, using optical imaging agents in particular, has already shown itself to be a boon to the research efforts to better understand the process. Unfortunately, owing to significant light scattering, widespread clinical application is not practical. Attempts to develop similar targeted MRI agents have been made, with the hopes of maintaining directed specificity while improving the spatial resolution. There has been little success in the clinical translation of such imaging agents, likely attributable to the intrinsically low sensitivity of MRI imaging (i.e., relatively large amounts of Gadolinium are required to obtain an adequate signal, making the chemistry and safety of these agents challenging).

The preclinical work using targeted US microbubbles is also promising. The ability to release a therapy payload 'on demand' suggests the possibility of a combined imaging and therapeutic paradigm. Labeling microbubbles with specific targeted molecules may result in an imaging agent platform similar to that in nuclear medicine and PET; however, compared with radionuclide imaging, US imaging requires a higher dose and further safety testing will be necessary for regulatory approval.

Radionuclide imaging alone is able to bridge the translational gap for targeted imaging, providing dynamic high sensitivity targeted

information, albeit with low spatial resolution, in both the preclinical and clinical arenas. Several angiogenesis-targeted PET imaging agents are already in clinical trials with promising results. While more safety and efficacy studies are needed, it is likely that an integrin-targeted PET imaging agent will be translated to the clinic in the next decade.

While the clinical implication of modulating angiogenesis is currently uncertain, given the major role it plays in various disease states, the ability to monitor angiogenesis noninvasively over time will be a useful medical tool in the near future. Theranostic platforms currently in development offer the potential to select, properly dose and monitor patients with therapies directed at angiogenesis.

#### Financial & competing interests disclosure

*While no monetary benefits have been received, the Molecular Imaging Program does have research agreements with Phillips Medical and GE Healthcare, and imaging agents have been provided free of charge from the latter.*

*The authors have no other relevant affiliations or financial involvement with any organization or entity with a financial interest in or financial conflict with the subject matter or materials discussed in the manuscript apart from those disclosed.*

*No writing assistance was utilized in the production of this manuscript.*

#### Bibliography

- Folkman J. Tumor angiogenesis: therapeutic implications. *N. Engl. J. Med.* 282(21), 1182–1186 (1971).
- Black WC, Welch HG. Advances in diagnostic imaging and overestimations of disease prevalence and the benefits of therapy. *N. Engl. J. Med.* 328(17), 1237–1243 (1993).
- Naumov GN, Akslen LA, Folkman J. Role of angiogenesis in human tumor dormancy: animal models of the angiogenic switch. *Cell Cycle* 16, 1779–1787 (2006).
- Folkman J. Angiogenesis. *Annu. Rev. Med.* 57, 1–18 (2006).
- Udagawa T, Fernandez A, Achilles EG, Folkman J, D'Amato RJ. Persistence of microscopic human cancers in mice: alterations in the angiogenic balance accompanies loss of tumor dormancy. *FASEB J.* 16(11), 1361–1370 (2002).
- Sinusas AJ. Molecular imaging in nuclear cardiology: translating research concepts into clinical applications. *Q. J. Nucl. Med. Mol. Imaging* 54(2), 230–240 (2010).
- Tumor Angiogenesis: Basic Mechanisms and Cancer Therapy.* Marmé D, Fusenig N (Eds). Springer-Verlag, Berlin, Germany (2008).
- Venkataraman G, Raman R, Sasisekharan V, Sasisekharan R. Molecular characteristics of fibroblast growth factor–fibroblast growth factor receptor–heparin-like glycosaminoglycan complex. *Proc. Natl Acad. Sci. USA* 96(7), 3658–3663 (1999).
- White CW, Sondheimer HM, Crouch EC, Wilson H, Fan LL. Treatment of pulmonary hemangiomas with recombinant interferon  $\alpha$ -2a. *N. Engl. J. Med.* 320(18), 1197–1200 (1989).
- Singh RK, Gutman M, Bucana CD, Sanchez R, Llansa N, Fidler IJ. Interferons  $\alpha$  and  $\beta$  down-regulate the expression of basic fibroblast growth factor in human carcinomas. *Proc. Natl Acad. Sci. USA* 92(10), 4562–4566 (1995).
- Beer AJ, Haubner R, Wolf I *et al.* PET-based human dosimetry of  $^{18}\text{F}$ -galacto-RGD, a new radiotracer for imaging  $\alpha\text{v}\beta 3$  expression. *J. Nucl. Med.* 47(5), 763–769 (2006).
- Smith-Jones PM, Solit D, Afroze F, Rosen N, Larson SM. Early tumor response to Hsp90 therapy using HER2 PET: comparison with  $^{18}\text{F}$ -FDG PET. *J. Nucl. Med.* 47(5), 793–796 (2006).
- Schwarz F, Sculean A, Romanos G *et al.* Influence of different treatment approaches on the removal of early plaque biofilms and the viability of SAOS2 osteoblasts grown on titanium implants. *Clin. Oral Investig.* 9(2), 111–117 (2005).
- Prandini MH, Denarier E, Frachet P, Uzan G, Marguerie G. Isolation of the human platelet glycoprotein IIb gene and characterization of the 5' flanking region. *Biochem. Biophys. Res. Commun.* 156(1), 595–601 (1988).
- Cai J, Han S, Qing R, Liao D, Law B, Boulton ME. In pursuit of new anti-angiogenic therapies for cancer treatment. *Front. Biosci.* 16, 803–814 (2011).
- Ignoffo RJ. Overview of bevacizumab: a new cancer therapeutic strategy targeting vascular endothelial growth factor. *Am. J. Health Syst. Pharm.* 61(21 Suppl. 5), S21–S26 (2004).

- 17 Batchelor TT, Sorensen AG, di Tomaso E *et al.* AZD2171, a pan-VEGF receptor tyrosine kinase inhibitor, normalizes tumor vasculature and alleviates edema in glioblastoma patients. *Cancer Cell* 11(1), 83–95 (2007).
- 18 Mas-Moruno C, Rechenmacher F, Kessler H. Cilengitide: the first anti-angiogenic small molecule drug candidate design, synthesis and clinical evaluation. *Anticancer Agents Med. Chem.* 10(10), 753–768 (2010).
- 19 Celik I, Surucu O, Dietz C *et al.* Therapeutic efficacy of endostatin exhibits a biphasic dose–response curve. *Cancer Res.* 65(23), 11044–11050 (2005).
- 20 Kerbel RS, Yu J, Tran J *et al.* Possible mechanisms of acquired resistance to anti-angiogenic drugs: implications for the use of combination therapy approaches. *Cancer Metastasis Rev.* 20(1–2), 79–86 (2001).
- 21 Sourbron S. Technical aspects of MR perfusion. *Eur. J. Radiol.* 76(3), 304–313 (2010).
- 22 Turkbey B, Shah VP, Pang Y *et al.* Is apparent diffusion coefficient associated with clinical risk scores for prostate cancers that are visible on 3-T MR images? *Radiology* 258(2), 488–495 (2011).
- 23 Mendichovszky IA, Cutajar M, Gordon I. Reproducibility of the aortic input function (AIF) derived from dynamic contrast-enhanced magnetic resonance imaging (DCE-MRI) of the kidneys in a volunteer study. *Eur. J. Radiol.* 71(3), 576–581 (2009).
- 24 Cutajar M, Mendichovszky IA, Tofts PS, Gordon I. The importance of AIF ROI selection in DCE-MRI renography: reproducibility and variability of renal perfusion and filtration. *Eur. J. Radiol.* 74(3), E154–E160 (2010).
- 25 Kummur S, Gutierrez ME, Chen A *et al.* Phase I trial of vandetanib and bevacizumab evaluating the VEGF and EGF signal transduction pathways in adults with solid tumours and lymphomas. *Eur. J. Cancer* 47(7), 997–1005 (2011).
- 26 Hayes DF. Bevacizumab treatment for solid tumors: boon or bust? *J. Am. Med. Assoc.* 305(5), 506–508 (2011).
- 27 Ranpura V, Hapani S, Wu S. Treatment-related mortality with bevacizumab in cancer patients: a meta-analysis. *J. Am. Med. Assoc.* 305(5), 487–494 (2011).
- 28 Padhani AR, Leach MO. Antivascular cancer treatments: functional assessments by dynamic contrast-enhanced magnetic resonance imaging. *Abdom. Imaging* 30(3), 324–341 (2005).
- 29 Zweifel M, Padhani AR. Perfusion MRI in the early clinical development of antivascular drugs: decorations or decision making tools? *Eur. J. Nucl. Med. Mol. Imaging* 37(Suppl. 1), S164–S182 (2010).
- 30 Ferrara KW, Merritt CR, Burns PN, Foster FS, Mattrey RF, Wickline SA. Evaluation of tumor angiogenesis with US: imaging, Doppler, and contrast agents. *Acad. Radiol.* 7(10), 824–839 (2000).
- 31 Pinter SZ, Lacefield JC. Detectability of small blood vessels with high-frequency power Doppler and selection of wall filter cut-off velocity for microvascular imaging. *Ultrasound Med. Biol.* 35(7), 1217–1228 (2009).
- 32 Martinoli C, Pretolesi F, Crespi G *et al.* Power Doppler sonography: clinical applications. *Eur. J. Radiol.* 27(Suppl. 2), S133–S140 (1998).
- 33 Chen CN, Cheng YM, Liang JT *et al.* Color Doppler vascularity index can predict distant metastasis and survival in colon cancer patients. *Cancer Res.* 60(11), 2892–2897 (2000).
- 34 Chen CN, Lin JJ, Lee H *et al.* Association between color doppler vascularity index, angiogenesis-related molecules, and clinical outcomes in gastric cancer. *J. Surg. Oncol.* 99(7), 402–408 (2009).
- 35 Zhou Q, Lei XY, Xie Q, Cardoza JD. Sonographic and Doppler imaging in the diagnosis and treatment of gestational trophoblastic disease: a 12-year experience. *J. Ultrasound Med.* 24(1), 15–24 (2005).
- 36 Cosgrove D, Lassau N. Imaging of perfusion using ultrasound. *Eur. J. Nucl. Med. Mol. Imaging* 37(Suppl. 1), S65–S85 (2010).
- 37 Magnon C, Galaup A, Rouffiac V *et al.* Dynamic assessment of antiangiogenic therapy by monitoring both tumoral vascularization and tissue degeneration. *Gene Ther.* 14(2), 108–117 (2007).
- 38 Eisenbrey JR, Forsberg F. Contrast-enhanced ultrasound for molecular imaging of angiogenesis. *Eur. J. Nucl. Med. Mol. Imaging* 37(Suppl. 1), S138–S146 (2010).
- 39 Lassau N, Koscielny S, Albiges L *et al.* Metastatic renal cell carcinoma treated with sunitinib: early evaluation of treatment response using dynamic contrast-enhanced ultrasonography. *Clin. Cancer Res.* 16(4), 1216–1225 (2010).
- 40 Kety SS. Observations on the validity of a two compartmental model of the cerebral circulation. *Acta Neurol. Scand. Suppl.* 14, 85–87 (1965).
- 41 Grubb RL Jr, Phelps ME, Ter-Pogossian MM. Regional cerebral blood volume in humans. X-ray fluorescence studies. *Arch. Neurol.* 28(1), 38–44 (1973).
- 42 Line BR, Mitra A, Nan A, Ghandehari H. Targeting tumor angiogenesis: comparison of peptide and polymer–peptide conjugates. *J. Nucl. Med.* 46(9), 1552–1560 (2005).
- 43 Sipkins DA, Cheresch DA, Kazemi MR, Nevin LM, Bednarski MD, Li KC. Detection of tumor angiogenesis *in vivo* by  $\alpha$ V $\beta$ 3-targeted magnetic resonance imaging. *Nat. Med.* 4(5), 623–626 (1998).
- 44 Haubner R, Wester HJ, Burkhart F *et al.* Glycosylated RGD-containing peptides: tracer for tumor targeting and angiogenesis imaging with improved biokinetics. *J. Nucl. Med.* 42(2), 326–336 (2001).
- 45 Haubner R, Wester HJ, Weber WA *et al.* Noninvasive imaging of  $\alpha$ (v) $\beta$ 3 integrin expression using  $^{18}$ F-labeled RGD-containing glycopeptide and positron emission tomography. *Cancer Res.* 61(5), 1781–1785 (2001).
- 46 Beer AJ, Niemeyer M, Carlsen J *et al.* Patterns of  $\alpha$  $\beta$  $\beta$  $\beta$  expression in primary and metastatic human breast cancer as shown by  $^{18}$ F-Galacto-RGD PET. *J. Nucl. Med.* 49(2), 255–259 (2008).
- 47 Beer AJ, Haubner R, Goebel M *et al.* Biodistribution and pharmacokinetics of the  $\alpha$  $\beta$  $\beta$  $\beta$ -selective tracer  $^{18}$ F-galacto-RGD in cancer patients. *J. Nucl. Med.* 46(8), 1333–1341 (2005).
- 48 Beer AJ, Haubner R, Sarbia M *et al.* Positron emission tomography using [ $^{18}$ F]galacto-RGD identifies the level of integrin  $\alpha$ (v) $\beta$ 3 expression in man. *Clin. Cancer Res.* 12(13), 3942–3949 (2006).
- 49 Haubner R, Kuhnast B, Mang C *et al.* [ $^{18}$ F]galacto-RGD: synthesis, radiolabeling, metabolic stability, and radiation dose estimates. *Bioconj. Chem.* 15(1), 61–69 (2004).
- 50 Haubner R. Av $\beta$ 3-integrin imaging: a new approach to characterise angiogenesis? *Eur. J. Nucl. Med. Mol. Imaging* 33(Suppl. 1), 54–63 (2006).
- 51 Makowski MR, Ebersberger U, Nekolla S, Schwaiger M. *In vivo* molecular imaging of angiogenesis, targeting  $\alpha$  $\beta$  $\beta$  $\beta$  integrin expression, in a patient after acute myocardial infarction. *Eur. Heart J.* 29(18), 2201 (2008).
- 52 Kenny LM, Coombes RC, Oulie I *et al.* Phase I trial of the positron-emitting Arg-Gly-Asp (RGD) peptide radioligand  $^{18}$ F-AH111585 in breast cancer patients. *J. Nucl. Med.* 49(6), 879–886 (2008).
- 53 Nielsen CH, Kimura RH, Withofs N *et al.* PET imaging of tumor neovascularization in a transgenic mouse model with a novel  $^{64}$ Cu-DOTA-knottin peptide. *Cancer Res.* 15 70(22), 9022–9030 (2010).

- 54 Wagner S, Fueller T, Hummel V, Rieckmann P, Tonn JC. Influence of VEGF-R2 inhibition on MMP secretion and motility of microvascular human cerebral endothelial cells (HCEC). *J. Neurooncol.* 62(3), 221–231 (2003).
- 55 Cai W, Chen K, Mohamedali KA *et al.* PET of vascular endothelial growth factor receptor expression. *J. Nucl. Med.* 47(12), 2048–2056 (2006).
- 56 Willmann JK, Chen K, Wang H *et al.* Monitoring of the biological response to murine hindlimb ischemia with <sup>64</sup>Cu-labeled vascular endothelial growth factor-121 positron emission tomography. *Circulation* 117(7), 915–922 (2008).
- 57 Rodriguez-Porcel M, Cai W, Gheysens O *et al.* Imaging of VEGF receptor in a rat myocardial infarction model using PET. *J. Nucl. Med.* 49(4), 667–673 (2008).
- 58 Nagengast WB, de Korte MA, Oude Munnink TH *et al.* <sup>89</sup>Zr-bevacizumab PET of early antiangiogenic tumor response to treatment with HSP90 inhibitor NVP-AUY922. *J. Nucl. Med.* 51(5), 761–767 (2010).
- 59 Nagengast WB, Lub-de Hooge MN, Oosting SF *et al.* VEGF-PET imaging is a noninvasive biomarker showing differential changes in the tumor during sunitinib treatment. *Cancer Res.* 71(1), 143–153 (2011).
- 60 Nayak TK, Garmestani K, Baidoo KE, Milenic DE, Brechbiel MW. PET imaging of tumor angiogenesis in mice with VEGF-A-targeted (86)Y-CHX-A”-DTPA-bevacizumab. *Int. J. Cancer* 128(4), 920–926 (2011).
- 61 Almutairi A, Rossin R, Shokeen M *et al.* Biodegradable dendritic positron-emitting nanoprobe for the noninvasive imaging of angiogenesis. *Proc. Natl Acad. Sci. USA* 106(3), 685–690 (2009).
- 62 Ellegala DB, Poi HL, Carpenter JE *et al.* Imaging tumor angiogenesis with contrast ultrasound and microbubbles targeted to  $\alpha(v)\beta(3)$ . *Circulation* 108(3), 336–341 (2003).
- 63 Xie F, Lof J, Matsunaga T, Zutshi R, Porter TR. Diagnostic ultrasound combined with glycoprotein IIb/IIIa-targeted microbubbles improves microvascular recovery after acute coronary thrombotic occlusions. *Circulation* 119(10), 1378–1385 (2009).
- 64 Willmann JK, Kimura RH, Deshpande N, Lutz AM, Cochran JR, Gambhir SS. Targeted contrast-enhanced ultrasound imaging of tumor angiogenesis with contrast microbubbles conjugated to integrin-binding knottin peptides. *J. Nucl. Med.* 51(3), 433–440 (2010).
- 65 Pysz MA, Foygel K, Rosenberg J, Gambhir SS, Schneider M, Willmann JK. Antiangiogenic cancer therapy: monitoring with molecular US and a clinically translatable contrast agent (BR55). *Radiology* 256(2), 519–527 (2010).
- 66 Anderson CR, Rychak JJ, Backer M, Backer J, Ley K, Klibanov AL. scVEGF microbubble ultrasound contrast agents: a novel probe for ultrasound molecular imaging of tumor angiogenesis. *Invest Radiol.* 45(10), 579–585 (2010).
- 67 Myrset AH, Fjerdningstad HB, Bendiksen R *et al.* Design and characterization of targeted ultrasound microbubbles for diagnostic use. *Ultrasound Med. Biol.* 37(1), 136–150 (2011).
- 68 Deshpande N, Pysz MA, Willmann JK. Molecular ultrasound assessment of tumor angiogenesis. *Angiogenesis* 13(2), 175–188 (2010).
- 69 Spuentrup E, Botnar RM. Coronary magnetic resonance imaging: visualization of the vessel lumen and the vessel wall and molecular imaging of arteriothrombosis. *Eur. Radiol.* 16(1), 1–14 (2006).